

# OPTIMIZATION OF XENON FLASHLAMP HEATING IN THERMOPLASTIC AUTOMATED FIBRE PLACEMENT

Michael Edwards, Andrew Page, David Williams, Anastasios Danezis,

Heraeus Noblelight Ltd,

Cambridge, UK

Michael Schilling, Torsten Jenek

Heraeus Noblelight GmbH,

Hanau, Germany

## ABSTRACT

As an alternative to infrared lamps and lasers, a new heating technology for composites manufacturing processes has emerged that is based on the Xenon flashlamp. In the Automated Fibre Placement (AFP) process, a pulsing Xenon flashlamp is used to heat the substrate and incoming tow before consolidation is achieved under a compaction roller. The Xenon flashlamp system has been shown to match the rapid response time of a laser and reach the temperatures required to process thermoplastic composites. Pulse parameters of energy, duration and frequency are varied during lay-up to account for changes in speed and geometry and maintain a target temperature. To optimize these parameters, an opto-thermal simulation model has been created that utilises optical ray tracing techniques to characterise the flashlamp source and finite element analysis (FEA) to predict the resultant processing temperature. Using these simulation tools, pulse parameters can be chosen to achieve a desired processing temperature without the need for physical trials. In this paper, the simulation process is described. The characterisation of the Xenon flashlamp source, using Goniometric and spectral irradiance measurements, is presented. The source characterisation is then used to determine the spectral energy levels, spatial distribution, and electrical-to-radiative energy efficiency of the source. The optical ray tracing analysis is then detailed, which calculates surface irradiance profiles on the composite tow and substrate that are used as input boundary conditions to the thermal simulation.

Corresponding author: michael.edwards@heraeus.com

## 1. INTRODUCTION

A pulsed Xenon flashlamp system has been developed for the AFP and filament winding composites manufacturing processes. This system has been shown to achieve rapid tape heating equivalent to that of a laser heating system. Detailed descriptions of the background

of the pulsed flashlamp systems can be found in previous publications [1], [2], [3]. As with other heat sources, determining suitable heating parameters for a given material, geometry and AFP system is a relatively complex process. For the flashlamp, there are three programmable pulse parameters: pulse duration, voltage (energy), and frequency. Currently, when using a new material, geometry or AFP system, an experimental determination of the power law relating process speed to heating power is required, which can be time-consuming in terms of setup and materials.

To make this process more efficient, optical-thermal simulation tools using an approach like [4] are being developed for pulsed Xenon flashlamp systems using commercial finite-element (ANSYS Mechanical) and ray tracing (TracePro) software packages. The overall simulation workflow and the parts of the workflow covered in this paper are shown in figure 1. The thermal simulation method is described in [5] and therefore is not covered in this paper. When looking at the overall simulation workflow, firstly, the optical aspect of the simulation is solved within ray tracing with the irradiance of the composite surfaces measured within the ray tracing package acting as inputs for the thermal simulation, after being scaled and having timings calculated according to pulse parameters. The thermal aspect is solved as a transient thermal simulation within the FEA package, calculating the expected processing temperature. The simulation tool provides a predicted processing temperature to the operator, so the time required for an operator to determine appropriate operating parameters is greatly reduced.

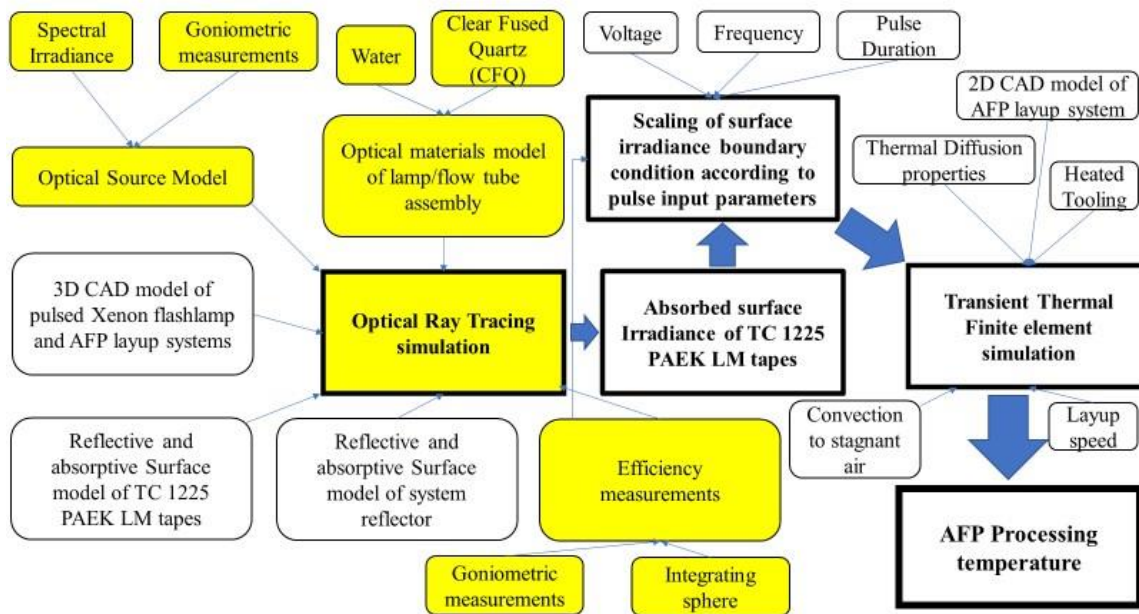


Figure 1. Optical-Thermal simulation workflow for a pulsed xenon flashlamp system. Highlighted areas in yellow are in the scope of this paper.

This paper concerns the optical characterisation work performed to produce a reliable optical ray tracing model for the thermal simulation. For the simulation tool to be accurate and useful to the system operator, it needs to be validated first optically and later thermally. In this paper, the optical validation of light exiting the pulsed Xenon flashlamp source and system head within the ray tracing simulation is described. Firstly, the spectral irradiance of the pulsed Xenon flashlamp source was measured and used as an input within the optical

simulation. The angular or goniometric distribution of light intensity from the source was measured to validate the distribution of light within the ray trace. The electrical-radiative energy conversion efficiency was investigated to determine the scaling and power levels required within the thermal simulation. Finally, the radiative energy exiting the system head was determined using an Integrating Sphere meaning the total efficiency of the system is known; this also means the internal flux threshold and ray splitting parameters within the optical model can be determined.

## 2. SPECTRAL IRRADIANCE MEASUREMENTS

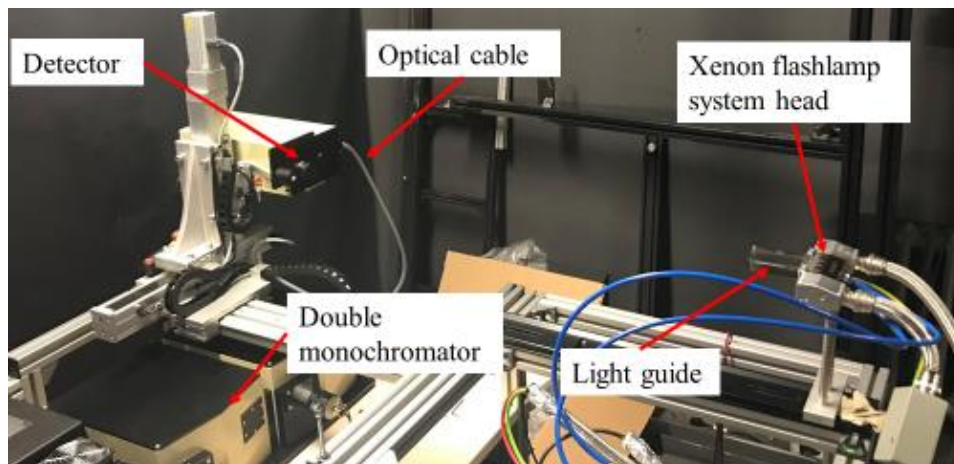
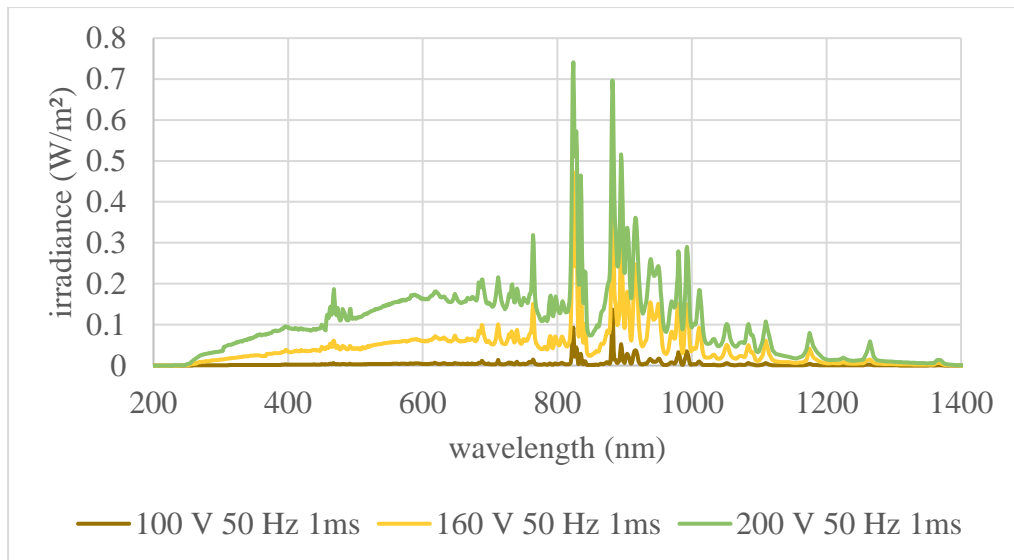
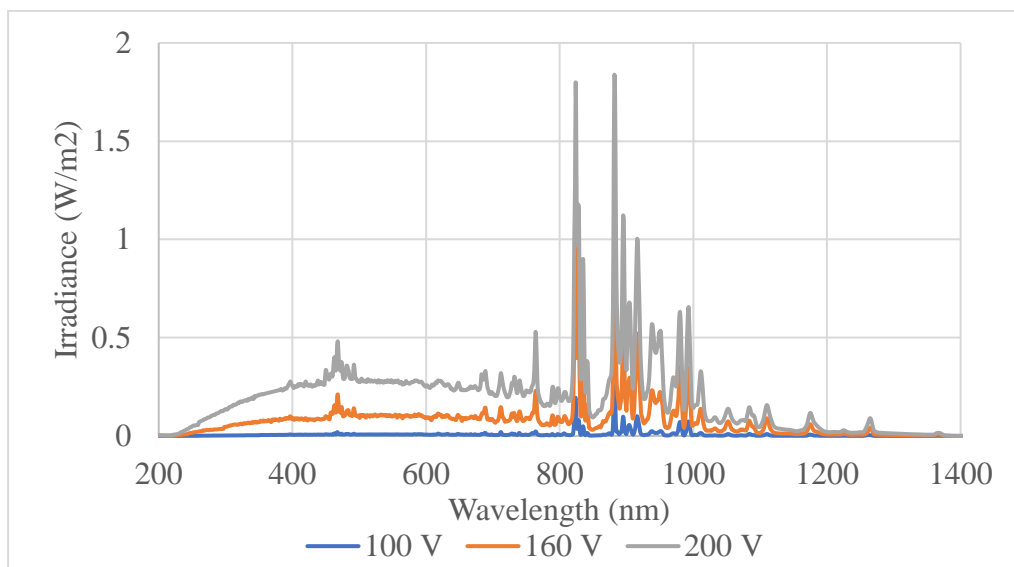


Figure 2. Image of double monochromator test setup used for spectral irradiance measurements

To determine the energy emission of a flashlamp with respect to wavelength via spectral irradiance measurements, the experimental setup shown in figure 2 has been devised. The system consists of a Xenon flashlamp within a water-filled clear fused quartz (CFQ) flow tube for cooling, mounted on a frame. A Bentham DTMC300 double monochromator was used to measure the spectral irradiance with sufficient detail. For this system the light from a source goes into a detector a pre-set distance away, typically 0.5 to 1 m, and the light is transported via an optical cable into the monochromator system. The double-monochromator then determines the light intensity at a specific wavelength. The system measures the intensity of light with respect to wavelength in 1 nm steps between 200 and 1100 nm, and at 5 nm steps between 1100 and 1700 nm. This results in a detailed spectral irradiance plot of the light source – in this case the entire emission curve of the Xe plasma is measured. The spectral emission measurement of both the ‘flashlamp with flow tube’, shown in figure 7 (b), and the ‘system head’, shown in figure 10 (a) are shown in figure 3. Figure 3 (a) shows typical behaviour for a Xenon flashlamp, with the proportion of UV energy increasing as the pulse energy (here represented by voltage) increases.



(a)



(b)

Figure 3. Spectral irradiance measurements at 100, 160 and 200 V of (a) a flashlamp head taken at 50 Hz frequency and 1ms pulse duration, at 1 m offset, (b) equivalent 'flashlamp with flow tube' at 50 Hz, 1ms and 0.5m offset.

## 2.1 Absorption of light within the lamp envelope and flow tube

Before detection by the double monochromator, for the 'flashlamp with flow tube' case, the rays pass through the two layers of Heraeus HLQ 200 clear fused quartz (CFQ) glass and the layer of water that constitute the lamp body and the flow tube itself. Since the spectral emission is broadband, it was prudent to check that these layers were not absorbing significant amounts of energy in the UV and IR regions. The attenuation coefficient,  $k$ , with respect to wavelength for water is available in the literature [6] and was calculated for the HLQ200 quartz from the transmission curves on the manufacturer's website [7]. The plots of  $k$  for both water and HLQ200 quartz are in figure 4 (a), with a plot of refractive indices in figure 4 (b). When including the  $k$  values

in absorption calculations, the energy losses to absorption are small in the 400 to 1000 nm range where most of the emissions occurs and, as figure 4 (c) shows, the correction to the irradiance of the optical model is subtle at this representative voltage level. The corrected spectral results in figure 4(c) have been included as a surface source model within the optical simulation.

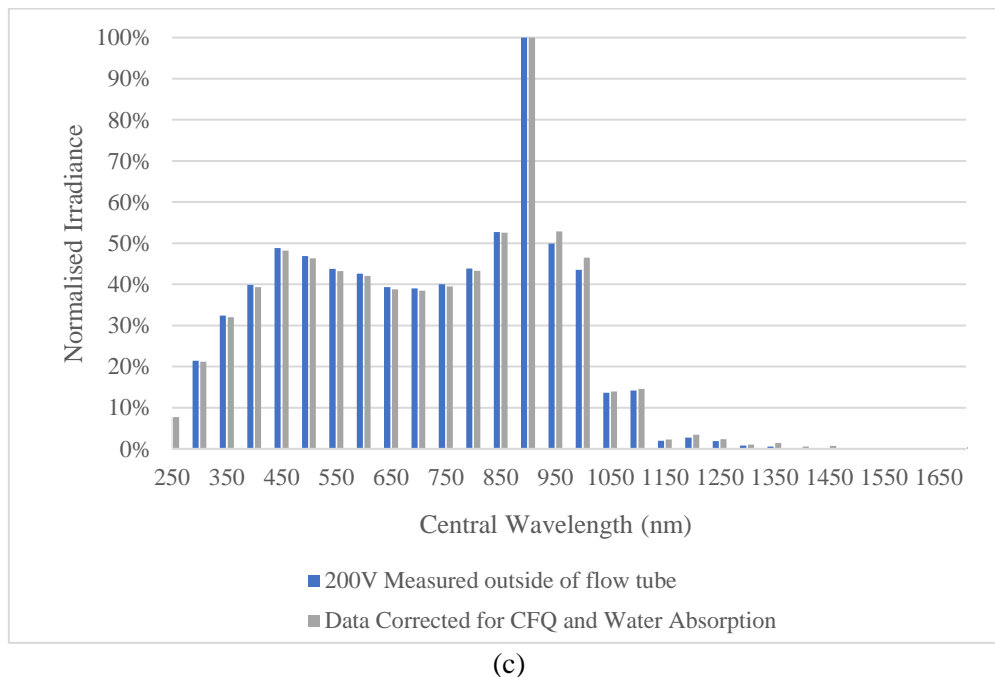
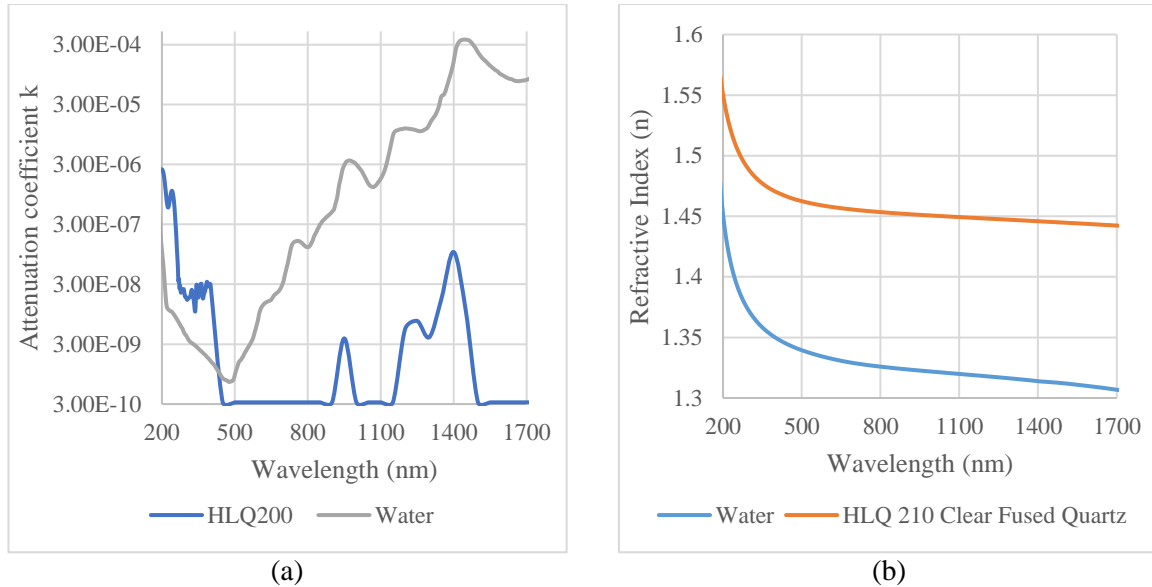


Figure 4. (a) Attenuation coefficient ( $k$ ) of water and HLQ 200 clear fused quartz (CFQ) used in the manufacturing for the xenon flashlamp and flow tube assembly. (b) Refractive indices of HLQ200 CFQ and water with respect to wavelength. (c) Absorption correction of both quartz and water applied to the Xenon flashlamp spectra used in the optical simulations.

### 3. GONIOMETRIC MEASUREMENTS

To determine the variation in intensity with respect to the angle from the source, the experimental setups shown in figure 5 were devised. To perform the goniometric measurements with the double monochromator, a manual rotational stage was added to the test set up as shown in figure 5 (b). The setup in figure 5 (a) uses a pyroelectric Gentec fluence ( $\text{J}/\text{cm}^2$ ) detector and the double monochromator is shown in figure 5 (b). The system consists of a Xenon flashlamp within a water-filled clear fused quartz (CFQ) flow tube mounted on a frame. This frame was attached to a rotational stage with a 30:1 gearbox that was controlled by a stepper motor. The rotational stage stepper motor was programmed to rotate in  $5^\circ$  intervals, with a pause of 2 or 5 seconds at each  $5^\circ$  increment. One to two metres away, as close to perpendicular to the plasma arc as reasonably possible, a pyroelectric Gentec fluence ( $\text{J}/\text{cm}^2$ ) detector was placed, set with a 24 mm diameter circular surface area. Multiple flashlamp pulses were measured at each angle. After measurements were taken (as the rotational stage timings were known) the data was filtered and averaged at each  $5^\circ$  angular increment for every single measurement. The measurements were converted from energy to fluence by dividing the value by the effective surface area of the measurement, which was  $4.5216 \text{ cm}^2$ , corresponding to the 24 mm diameter detector.

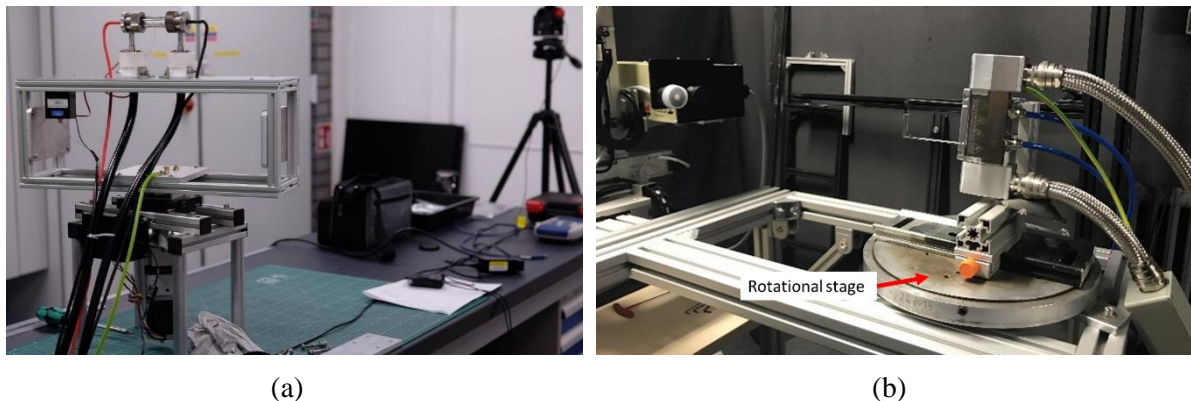


Figure 5. (a) Image of lamp on rotational stage with the Gentec detector and filter wheel in the background at 2m working distance. (b) Image of the pulsed xenon flashlamp system head on a manual rotational stage with the double monochromator 0.5 m away.

Goniometric measurements performed by both methods are displayed in figure 6. All measurements were normalised to investigate angular energy distribution rather than absolute power output at this point. Absolute power levels were used to calculate the optical efficiency of the flashlamp/flow tube system shown in table 1 and described later in this paper. The voltage was varied between 140 and 200 V for the pyroelectric measurements, whilst the measurements by double monochromator were only performed at 200 V as this method was more complicated and expensive. As figure 6 shows, the normalised angular distribution of energy for all voltage levels measured using the Gentec detector and double monochromator match closely. These measurements suggest that the Xenon source emits light in a cosine angular distribution defined as a Lambertian volume emitter [8]. The concentration of light at lower angles caused by diffraction results from light passing through the flow tube; this was confirmed by analysis in section 4.

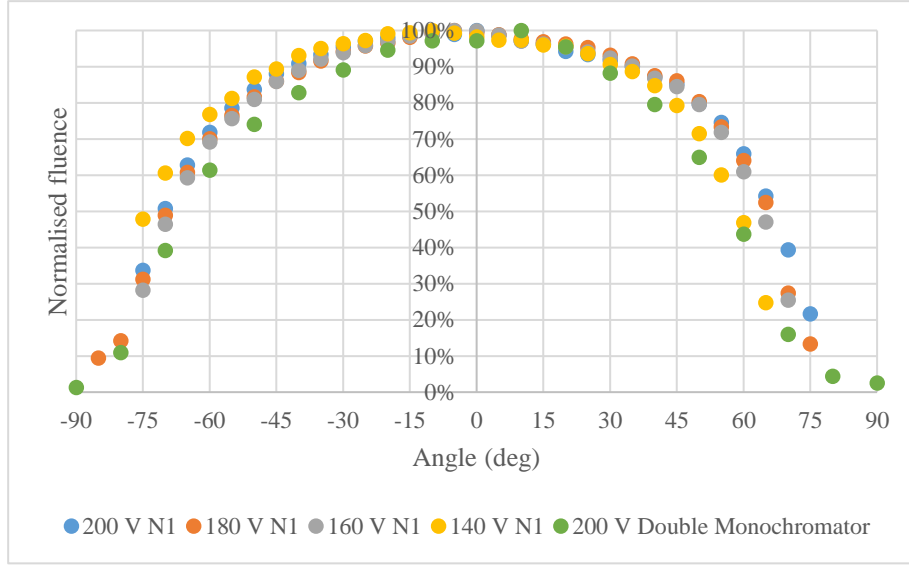


Figure 6. Normalised Horizontal Rotational Stage Results for measurements taken with the Gentec pyroelectric detector at 140, 160, 180 and 200 V, as well as a goniometric measurement taken with the double monochromator at 200 V.

### 3.1 Electrical to Optical Energy Efficiency

A preferable way to estimate power output and energy efficiency is to calculate the optical power output from the goniometric measurements of the Xenon flashlamp system head and ‘flashlamp with flow tube’ cases respectively. The mathematical relationship between irradiance ( $E$ ) and optical power ( $\varphi$ ) is given by.

$$E = \frac{\partial \varphi}{\partial A} \quad (1)$$

Where  $A$  is the surface area of the detection region. Taking the surface area to be a sphere with the flashlamp at its centre, and changing to polar coordinates, the equation becomes:

$$E = \frac{\partial \varphi}{r^2 \partial \theta \partial \phi} \quad (2)$$

Rearranging (2) into an integral for the spherical case with rotational symmetry about the rotational axis of a cylinder (as seen with the ‘lamp with flow tube’ setup) gives:

$$\varphi = r^2 \int_{-\pi}^{\pi} \partial \phi \int_{-\pi/2}^{\pi/2} E_{\theta} \partial \theta \quad (3)$$

Using the relationship in equation (3) and the previous goniometric measurements, it was possible to calculate the electrical-to-optical efficiency of the lamp with flow tube assembly,

as shown in table 1. The electrical pulse energy was determined from the current-voltage (IV) characteristics of a pulse measured by an oscilloscope.

As table 1 shows, the energy efficiency is around 40% for all flashlamp energy levels. This value is likely a small under-estimate of the ultimate energy conversion efficiency, as the pyroelectric detector absorbs only 98% of the optical energy and also the layers of water and quartz in the ‘flashlamp with flow tube’ assembly absorb a small amount of optical energy, as described previously.

Table 1. Calculation of electrical-to-radiative energy efficiency for different flashlamp voltage levels.

Calculated system power	200 V 1 ms Measurement	180 V 1 ms Measurement	160 V 1 ms Measurement	140 V 1 ms Measurement
Calculated initial electrical pulse energy	30.6 J	21.25 J	14.22 J	8.76 J
Total optical pulse energy exiting the flow tube	12.08 J	8.44 J	5.60 J	3.50 J
% of Initial Energy exiting the flow tube	39.4%	39.7%	39.4%	40.0%

#### 4. VALIDATION OF RAY TRACING SIMULATIONS

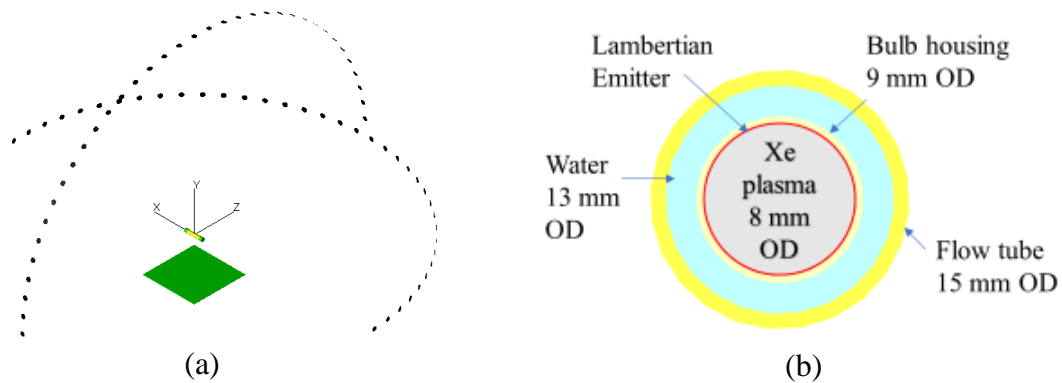


Figure 7. Schematic diagrams of the rotational stage ray trace. (a) full image of the ray trace model including the horizontal and vertical detectors. (b) Close-up of flashlamp and flow tube layers with outer diameter dimensions

To complement the rotational stage measurements, an optical ray tracing model was created within TracePro. Schematic diagrams of the ray tracing model are shown in figure 7. A flow tube model was created within TracePro using the dimensions for the flashlamp model as shown in figure 7 (b). A perfectly absorbing circular exit surface was placed 1m away from the centre of the flashlamp in the same position as the pyroelectric detector in the physical

measurements. Further identical detectors were created at 5° intervals until there was 180° coverage in the horizontal and vertical directions, as shown in figure 7 (a). The Xenon plasma was simulated as a cylindrical Lambertian emitter with a cylinder diameter of 7.96 mm and cylinder length of 70 mm, which corresponds to an 8 mm bore lamp and 70mm arc length respectively. To get sufficient convergence at the detectors 1 m away, the cylindrical emitter model was set to produce  $2 \times 10^7$  rays.

#### 4.1 Comparison with Horizontal Goniometric Measurements

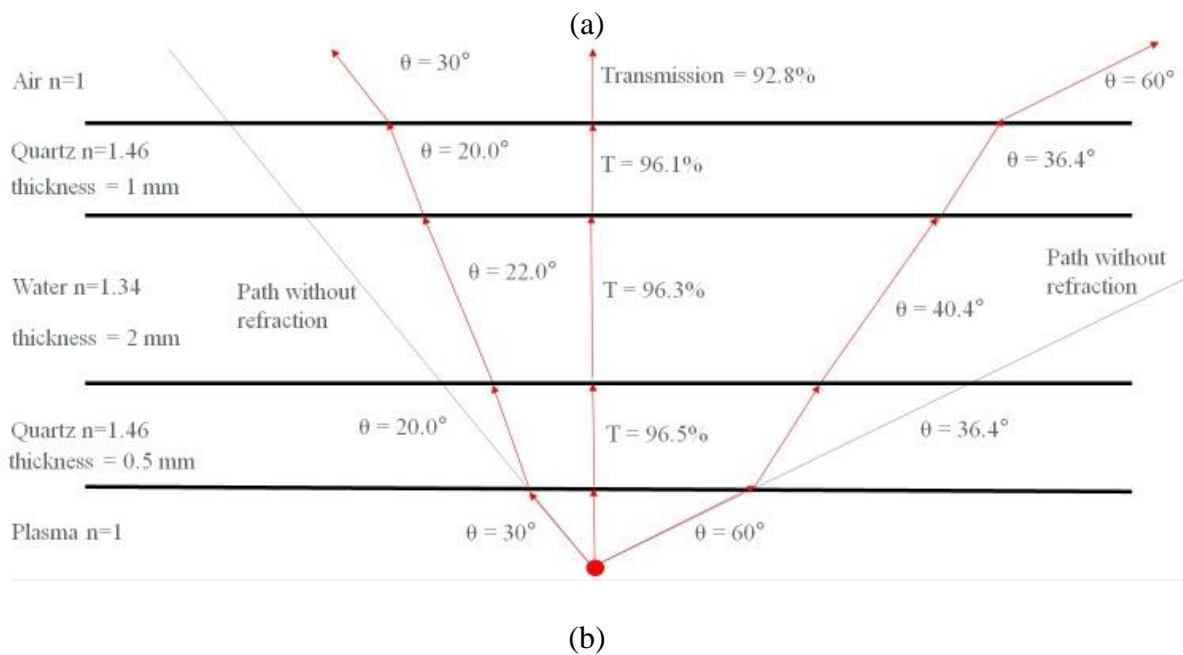
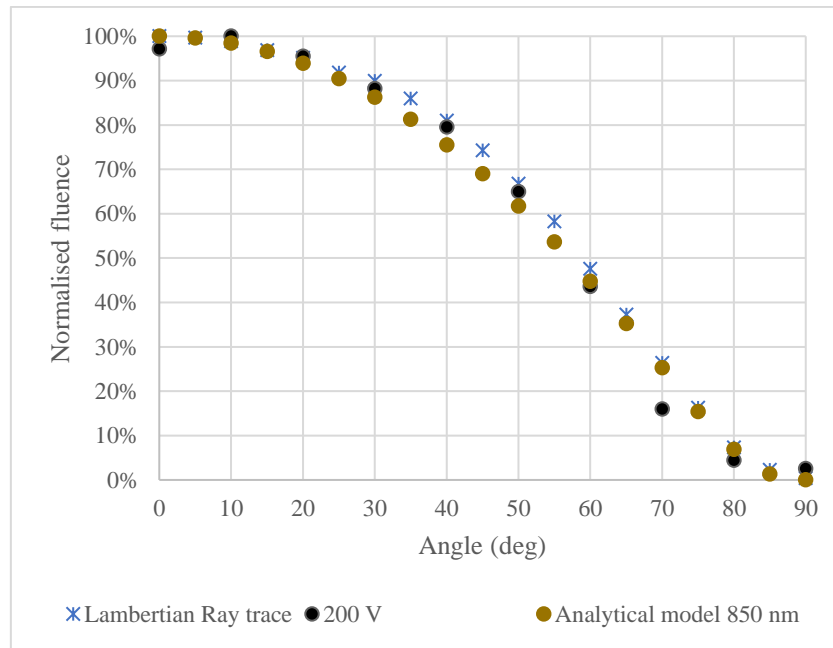


Figure 8. (a) Normalised comparison between the goniometric measurement of the ‘lamp with flow tube’ setup measured at 200V 50Hz 1ms with a ray trace of a Lambertian

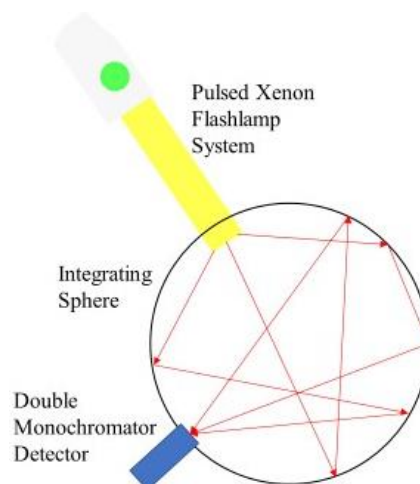
volume emitter and a 2D analytical model of a Lambertian point source with rays passing through the flashlamp/flow tube assembly. (b) Ray diagram of 850 nm wavelength rays leaving a point source at 0, 30 and 60°, demonstrating the concentration of light seen for the flashlamp/flow tube assembly at lower angles.

The results in figure 8 suggest a Lambertian source with the angular intensity concentrated towards the lower angles by diffraction determined by Fresnel's equations [8]. This gives a strong indication that the light source is indeed very close to Lambertian and the current modelling assumption of a perfect Lambertian emitter is valid in the polar direction. To further understand this behaviour, a 2D analytical model of a Lambertian point source with rays passing through three media, firstly a 0.5 mm thick quartz layer representing the lamp housing, then a 2 mm water layer including absorption properties and finally a 1 mm quartz layer representing the flow tube was assessed. The analytical model includes the wavelength-dependent attenuation coefficients and refractive indices for both quartz and water, representing the lamp housing and flow tube materials, as shown in figure 4 (a-b). The wavelength dependent refractive index of the quartz was calculated using the Sellmaier equation using the coefficients given in [9]. For the example shown in figure 8, a wavelength of 850 nm was selected as it is the midpoint of the region of highest spectral intensity shown in figure 4 (c). This analytical model has been expanded to the entire range of flashlamp wavelengths and includes the absorption data shown in figure 4 (a). The excellent agreement between the ray trace and analytical model acts to validate the ray tracing model and shows that the simulation approach for the flashlamp/flow tube assembly, where the Xenon plasma is treated as a Lambertian volume emitter, is valid.

## 5. ENERGY EXITING THE SYSTEM HEAD



(a)



(b)

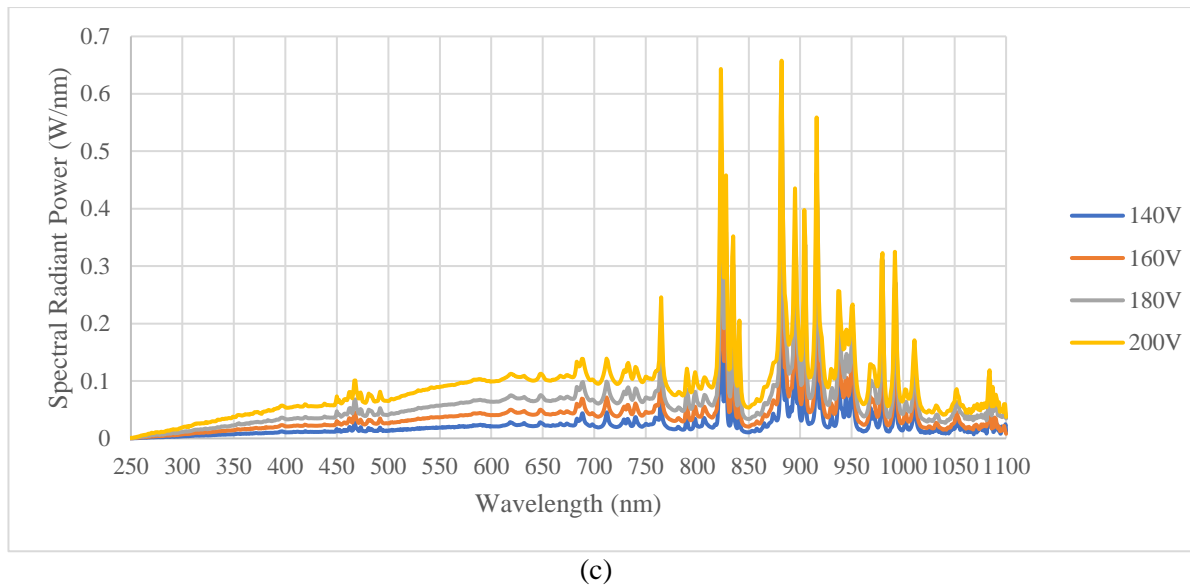


Figure 9. (a) Image of the Integrating Sphere used for the measurements. (b) Schematic diagram showing the experimental setup. (c) Spectral radiant power measurements taken by the integrating sphere at 10 Hz 1ms between 140 and 200 V set voltage

As a final calibration step for the optical system model, the total energy emitted at wavelengths between 250 and 1100 nm from the end of the pulsed Xenon flashlamp system quartz lightguide was measured using an integrating sphere with a static double monochromator detector attached. A schematic of the integrating sphere test setup is shown in figure 9. An integrating sphere consists of a diffuse spherical reflector with an aperture containing the double monochromator detector and an opening for the light guide. As the diffuse reflecting surface reflects close to 100% of the light, it makes it possible to collect almost the entirety of the light emitted from the source at the detector within the wavelength range.

Table 2. Optical Efficiency estimations of pulsed xenon flashlamp system between 140 V and 200 V.

Set Voltage (V)	Measured Wattage 250 to 1100 nm (W)	Corrected Wattage 250 to 1700 nm (W)	Optical Pulse Energy (J)	Exiting Pulse Energy (J)	Optical Efficiency of rays from the Flashlamp/Flow Tube Assembly to Exiting the Head
140	21.84	22.99	3.5	2.30	65.68%
160	36.97	38.92	5.6	3.89	69.50%
180	54.30	57.16	8.44	5.72	67.72%
200	78.75	82.90	12.08	8.29	68.62%
<b>Predicted Optical Efficiency of Ray Tracing Simulation</b>					<b>68.02%</b>

Firstly, the minimum pulse repetition rate of the detector was determined to be 10 Hz, and this was an improvement on the larger range Bentham detector, which had to run at 50 Hz and above for 1 ms pulses; with the measurements shown in figure 9 (c). The top wavelength

of 1100 nm meant that all emissions above 1100 nm were missing from the final analysis and the missing emissions were determined to be close to 5% of the total at both 160 and 200 V, based on the spectral irradiance measurements shown in figure 3 (a) and supplemental measurements. Based on these calculations and the information in table 1, it was possible to estimate the proportion of rays that were measured exiting the system head compared to the original ‘flashlamp with flow tube assembly’. This quantity is referred to as the “optical efficiency” for the purpose of this work. The results from the optical efficiency calculations are shown in table 2 and suggest an optical efficiency between 65.6 and 69.5%.

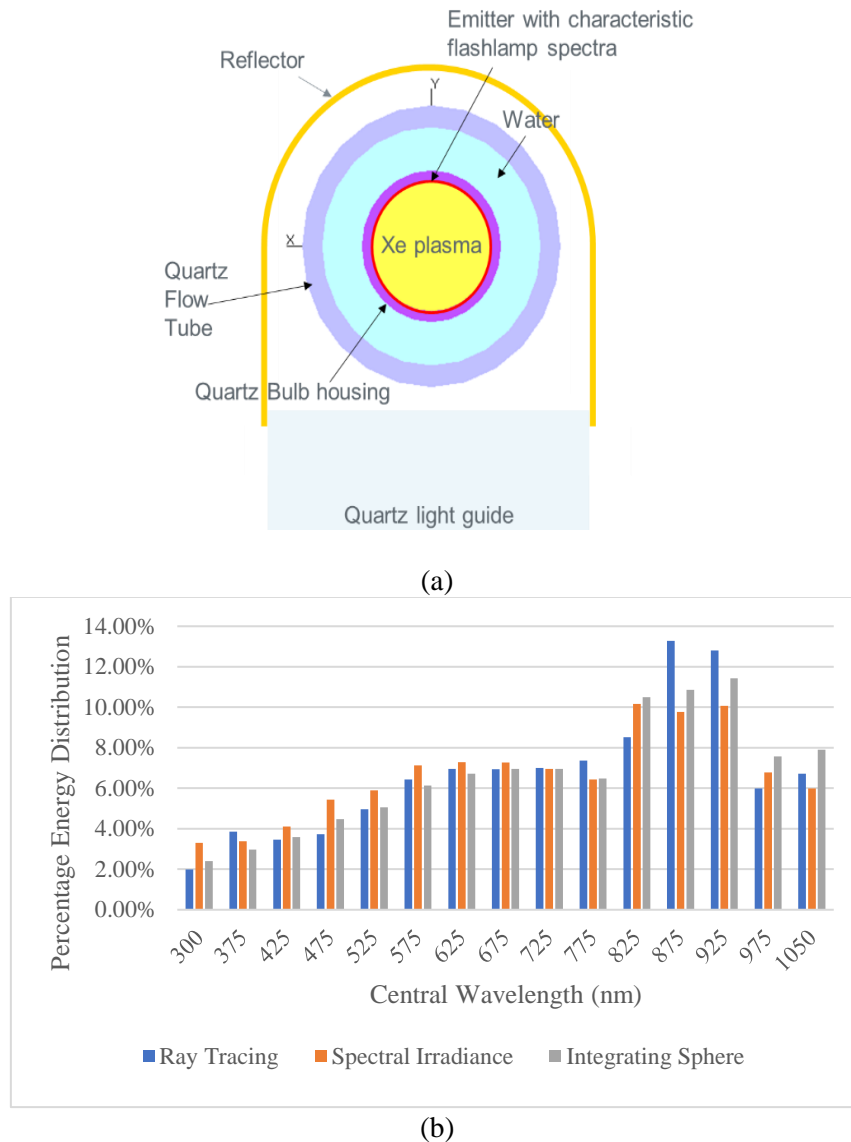


Figure 10. (a) Schematic of the pulsed xenon flashlamp system model. (b) Percentage energy distribution of light exiting the flashlamp system at 200V from the ray trace, spectral irradiance measurement in figure 4 (a) and integrating sphere in figure 9 (c).

In parallel to the integrating sphere measurements, an optical model of the pulsed Xenon flashlamp system was created within TracePro as shown in figure 10 (a). The optical model was designed to be as geometrically close to the actual flashlamp system as reasonably possible, but some simplifications around the lamp model and reflector were needed to avoid

issues with intersecting geometries within the optical simulation. The lamp model simplification is the same used for the goniometric validation model shown in figure 7 (b) and has therefore been shown to be valid. The plasma is assumed to be non-absorbing (optically thin) and have a refractive index of 1 - based on analysis of the optical opacity of Xenon plasmas with respect to wavelength at different current densities in [10] an optically thin plasma is a reasonable assumption. The spectral data used for the Lambertian emitter at the outer surface of the plasma cylindrical volume is the absorption corrected data at 200V in figure 4 (c). The light guide is assumed to be a generic fused silica (quartz) from the TracePro library [11]. Finally, the reflector is modelled as a specular reflective surface using appropriate parameters from [12].

Since all rays pass through several media of differing refractive indices the default TracePro setting of ray splitting enabled and a 5% threshold was found to be unsuitable. At these values, the reflected light component at the interface of two differing media with reasonably close refractive indices, such as quartz and water, would be removed from the simulation as this component would have a value less than 5% of the original ray. At the end of the solve, the result was a significant artificial loss of 28% of the original energy due to the flux threshold parameter. It was found that reducing the flux threshold value to an acceptable value from the energy loss perspective, whilst enabling ray splitting, was computationally expensive. Furthermore, there were no scattering properties within the simulation, the number of initial rays was set at  $10^6$  and the results from reducing the flux threshold were converging towards the ray splitting disabled result. Ray splitting was therefore disabled, meaning that the ray trace has the diffraction behaviour of an individual ray being determined probabilistically.

The ray tracing simulation predicts that 97.8% of the original optical rays exit the lamp/flow tube assembly. This is due to limited absorption of UV and IR energy by the water layer and very small losses in the UV region from the quartz layers. The simulation then predicts that 66.64% of the original optical energy exits the light guide into the integrating sphere. Therefore, the ratio of energy leaving the lamp/flow tube assembly to light exiting the full system into the integrating sphere, which is the same as the “optical efficiency” defined earlier, is 68.02% and this value falls in the range given in table 2. Finally, figure 10 (b) shows that the energy distribution of the light exiting the flashlamp system in the ray trace is broadly like the spectral irradiance and integrating sphere measurements. Agreement is excellent in the visible part of the spectrum where measurement is more reliable. The areas of most significant variation occur below 350 nm where measurement is difficult and between 800 and 1000 nm where there exist at least 12 visible emission lines and measuring the exact magnitude and position of these peaks is very difficult for a pulsed source. Considering the large number of emission lines will cause variability between results, the agreement between optical model and experiment is excellent. Therefore, this optical model is suitable for the optimisation of AFP layup by a pulsed Xenon flashlamp in conjunction with a thermal model developed with the methodology described in [5].

## 5.1 Predicted Losses in the System

The optical simulation contains data of optical behaviour of every ray striking the reflective surface and bulk material within the model. Since the pulsed flashlamp optical simulation has

been shown to produce results close to what is seen experimentally, further analysis can show where the system loses energy with the hope of creating a more optically efficient system. Table 3 contains the losses data for the optical simulation and demonstrates there are two key areas of losses, namely losses through absorption in the reflector block and water within the flow tube. De-ionised water is critical for the operation of the system as it cools the flashlamp during operation and allows it to be operated at higher power levels, more than offsetting any absorption losses. The simulation predicts that a quarter of the initial optical energy is lost within the reflector block, where most of this energy is absorbed and necessitating the need to water cool the reflector block in addition to the flow tube. Future investigations will look at the optical optimisation of the reflector block design and alternative reflector materials. Optimisation of the reflector design and investigation of alternative reflector materials can offer improved system efficiency, reducing the need for cooling and increasing the energy available for AFP layup. Increasing the energy for AFP layup will lead to improved consolidation or consolidation at a higher tape speed, leading to better material quality and/or higher throughput depending on the end user's needs.

Table 3. Analysis of predicted energy losses within the pulsed xenon flashlamp system

<b>Component</b>	<b>Percentage of Energy lost</b>
Lamp housing	0.02%
Water	6.9%
Flow tube	0.04%
Reflector Block	25.1%

## 6. CONCLUSION

An optical ray tracing model of a pulsed Xenon flashlamp system has been created within commercial ray tracing software and validated through spectral irradiance, goniometric and integrating sphere measurements. Estimates for overall and optical energy efficiencies have been calculated for this system and these values correlate well with the optical model. This means that power levels for the heat flux boundary condition within the thermal simulation can now be determined from the initial system pulse parameters of voltage, frequency, and pulse duration. The validation of the optical model brings the realisation of a simulation tool for the AFP layup of thermoplastics with a pulsed Xenon flashlamp source closer to reality and offers the potential to make further generations of the system more optically efficient with more output power available for the end user.

## 7. ACKNOWLEDGEMENTS

This project has received funding from the Clean Sky 2 Joint Undertaking under the European Union's Horizon 2020 research and innovation programme under grant agreement No 886549.

## 8. REFERENCES

- [1] Brown M., Monnot P., and Williams D., “Developments in Xenon flashlamp heating for automated fibre placement.” *In: Fourth International Symposium on Automated Composites Manufacturing*, Montreal, 2019.
- [2] Monnot P., Williams D., and Francesco M., “Power Control of a Flashlamp-based Heating Solution for Automated Dry Fibre Placement”. *In: 18th European Conference on Composite Materials*. Athens, 2018.
- [3] humm3™ - Intelligent heat for Automated Fibre Placement (AFP). <[https://www.heraeus.com/en/hng/products\\_and\\_solutions/arc\\_and\\_flash\\_lamps/humm3/humm3.html](https://www.heraeus.com/en/hng/products_and_solutions/arc_and_flash_lamps/humm3/humm3.html)>; May 2021
- [4] Stokes-Griffin C. M., and Compston P., “A combined optical-thermal model for near-infrared laser heating of thermoplastic composites in an automated tape placement process”, *Composites Part A: Applied Science and Manufacturing*, 75, (2015), p.104–15.
- [5] Danezis A., Williams D., Edwards M., and Skordos A. A., “Heat transfer modelling of flashlamp heating for automated tape placement of thermoplastic composites”, *Composites Part A: Applied Science and Manufacturing*, 145, (2021), 106381.
- [6] Hale G. M., and Querry M. R., “Optical Constants of Water in the 200-nm to 200- $\mu$ m Wavelength Region”, *Applied Optics*, 12 (3), (1973), p.555 – 563.
- [7] Heraeus Conamic - Transmission Calculator for Lamp Applications / Lamp Manufacturing  
<[https://www.heraeus.com/en/hca/fused\\_silica\\_quartz\\_knowledge\\_base\\_1/t\\_calc\\_1/transmission\\_calc\\_lamp/transmission\\_calculator\\_lm.html](https://www.heraeus.com/en/hca/fused_silica_quartz_knowledge_base_1/t_calc_1/transmission_calc_lamp/transmission_calculator_lm.html)>; May 2021
- [8] Yu F. T. S., and Yang X., *Introduction to Optical Engineering*, 1<sup>st</sup> Edition, 1997, Cambridge University Press, ISBN: 0-521-57493-5.
- [9] Quartz Glass for Optics: Data and Properties, Heraeus Conamic, Accessed from <[https://www.heraeus.com/media/media/hca/doc\\_hca/products\\_and\\_solutions\\_8/optics/Data\\_and\\_Properties\\_Optics\\_fused\\_silica\\_EN.pdf](https://www.heraeus.com/media/media/hca/doc_hca/products_and_solutions_8/optics/Data_and_Properties_Optics_fused_silica_EN.pdf)>; May 2021
- [10] Emmett J. L., Schawlow A. L., and Weinberg E. H., “Direct Measurement of Xenon Flashtube Opacity”, *Journal of Applied Physics* 35, 2601-2604 (1964)  
<https://doi.org/10.1063/1.1713807>
- [11] TracePro®. <[www.lambdare.com/tracepro/](http://www.lambdare.com/tracepro/)>; 2018.
- [12] Rakić A. D., Djurisić A. B., Elazar J. M., and Majewski M. L., “Optical properties of metallic films for vertical-cavity optoelectronic devices”, *Applied Optics* 1998; 37 (22): 5722-83.